In situ nucleoprotein structure involving origin-proximal SV40 DNA control elements

Li Zhang and Jay D.Gralla*
Department of Chemistry and Biochemistry and the Molecular Biology Institute, University of California, 405 Hilgard Avenue, Los Angeles, CA 90024-1569, USA

Received December 4, 1989; Revised and Accepted February 25, 1990

ABSTRACT

Nucleoprotein structures at the SV40 GC-box and adjacent AT-rich region have been probed by nucleases in permeabilized cells at nucleotide level resolution. The patterns of nuclease protection and hypersensitivity in these permeabilized cells that allow initiation of RNA and DNA synthesis are quite different from those observed in isolated nuclei that are inactive. Whereas simple DNA protection by factors is found in nuclei, the pattern in permeabilized cells includes very strong nuclease hypersensitive sites. Their arrangement suggests that the region exists as a higher order nucleoprotein complex *in vivo*, which is disturbed during the preparation of nuclei. The pattern is also found to be disturbed in permeabilized cells when T-antigen is inactivated by temperature-sensitive mutation. Since T-antigen origin binding sites and the GC-box region have been shown previously to interact functionally, the existence of a higher order structure involving both components provides a likely physical basis for the functional interaction of separate control elements.

INTRODUCTION

DNA control signals in animal cells usually consist of numerous elements that are not necessarily contiguous. The elements appear to be recognized individually by proteins but further communication between the elements is necessary for function. One possible molecular basis for this communication is the assembly of the separate proteins into a higher order nucleoprotein complex. Such a complex assembles at the SV40 major late promoter (1). SV40 nucleoprotein complexes are likely relevant to cellular transcription and replication regulation since the virus uses the host monkey cell machinery to replicate and transcribe its genome (2−5).

Cellular proteins and the viral T-antigen control transcription and replication by interacting with DNA sequences within an approximately 400 base pair region (6). During the late phase of the viral life cycle the elements at the edges of this 400 bp region assume prominent roles (6−9). It is at the late side edge that a nucleoprotein complex assembles over the late promoter elements. At the early side edge, ori sequences are required for viral DNA replication (6−9). One purpose of the experiments in this paper is to test whether a nucleoprotein complex assembles here as well.

Between these edges lie sets of accessory control elements, the six-fold redundant GC-boxes and the two-fold redundant enhancer element. These redundant control elements are multi-functional in that they influence both DNA replication and RNA transcription (8−15). Numerous protein factors have been isolated that bind to specific DNA sequences within the regulatory DNA (see 16 for example). However, these *in vitro* experiments have not yet reconstructed appropriately regulated replication and transcription systems.

As a complement to these ongoing *in vitro* reconstruction experiments, *in situ* probing experiments have revealed SV40 nucleoprotein complexes at the major late promoter (1) and within the GC-box region (17). This latter result was obtained from DNase I protection studies in SV40-infected isolated nuclei, where programmed factor binding fills the GC-boxes as the lytic cycle proceeds (17,18) By contrast, probing the late promoter region in permeabilized cells showed evidence of both protecting factors and higher order nucleoprotein structures, the latter being indicated by periodically arrayed nuclease hypersensitive sites. Since permeabilized CV-1 cells but not isolated nuclei retain the ability to initiate nucleic acid synthesis (19−21), we decided to re-investigate the interactions in the GC-box region using permeabilized cells as well as newly developed reagents. The proximity of the GC-boxes to the replication origin is important both for nucleic acid synthesis and chromatin structure (22). The results of these experiments suggest that a higher order structure connects the GC-box and the replication origin region, providing a plausible rationale for the known functional interaction between these separate control elements.

MATERIALS AND METHODS

Materials. Primer 5230 (TACTTCTGGAATAGCTC), which hybridizes to the early mRNA template strand from nt 5214 to 5230, was synthesized at the UCLA Facility. Micrococcal nuclease and deoxyribonuclease I were purchased from Worthington Biochemical Corp.; Klenow fragment was

* To whom correspondence should be addressed

purchased from Bethesda Research Laboratories and lysolecithin (type I) was purchased from Sigma. Mutant SVp7, in which the DNA from nt 32 to nt 73 in wt SV40 is deleted, was provided by R.L. Buchanan and J.D. Gralla. Temperature-sensitive mutant tsA58 was originally obtained from P. Tegtmeyer.

Treatment of Lysolecithin Permeabilized Cells with DNase I and MNase. This procedure has been described (1). Briefly, CV-1 cells were infected with 1−10 pfu/cell wild-type SV40 strain 776 or SVp7 or tsA58 and maintained in DMEM plus 2% calf serum in 10-cm-diameter plates. At 40 h post-infection, cell monolayers were treated with 0.5 mg/ml lysolecithin in solution A (150 mM sucrose, 80 mM KCl, 35 mM Hepes, pH 7.4, 5 mM potassium phosphate, 5 mM $MgCl_2$, 0.5 mM $CaCl_2$) for 1 min at 37°C. For tsA virus, incubation was for 68 h at 32.5°C followed by a 5 h treatment at 41°C when probing at the non-permissive temperature. Next, the lysolecithin solution was removed by aspiration and the cell monolayers were washed with solution A, and 1 ml of DNase I (approximately 0.1 mg/ml) in solution B (solution A with 80 mM of NaCl instead of KCl and with 2 mM $CaCl_2$) or MNase (250−500 units/ml) in solution C (150 mM sucrose, 50 mM Tris-HCl, pH 7.5, 50 mM NaCl, and 2 mM $CaCl_2$) was then added for 2 min at 37°C, or at 32.5°C for probing tsA58 at the permissive temperature. The enzyme solution was aspirated off the plates, and Hirt lysis solution (23) was added immediately to quench the residual DNase I or MNase activity. In other experiments, NP-40 nuclei were prepared and probed with DNase I as described (17). Finally, SV40 DNA was purified and probed with primer as described (17).

Treatment of Intact SV40-infected CV-1 Cells with $KMn0_4$. At 40 h post-infection, CV-1 cells were washed with phosphate-buffered saline (PBS). Approximately 10 mM $KMn0_4$ in PBS was then added for 1 min. The cells were scraped off the plates and spun down, then the residual $KMn0_4$ was quenched with 1 M β-mercaptoethanol and the Hirt lysis solution was added. SV40 DNA was then purified as described (17). This procedure has been described (1).

Primer Extension and Gel Electrophoresis. The sites of DNase I or MNase nicking or $KMn0_4$ modification were determined by hybridizing 5′-^{32}P-end labeled primers to denatured samples and extending to the sites of nicks or modification as described (17,24,25). Briefly, about 300,000 cts/min of end-labeled primer was added to the isolated DNA, followed by NaOH to bring the pH to 11. The DNA was then denatured by heating to 80°C for 2 min. After neutralization, primer 5230 was hybridized at 50°C for 3 min and extended with Klenow DNA polymerase at 50−52°C for 10 min. The DNA samples were then precipitated with ethanol and analyzed by 6% (w/v) acrylamide/50% (w/v) urea DNA sequencing gels.

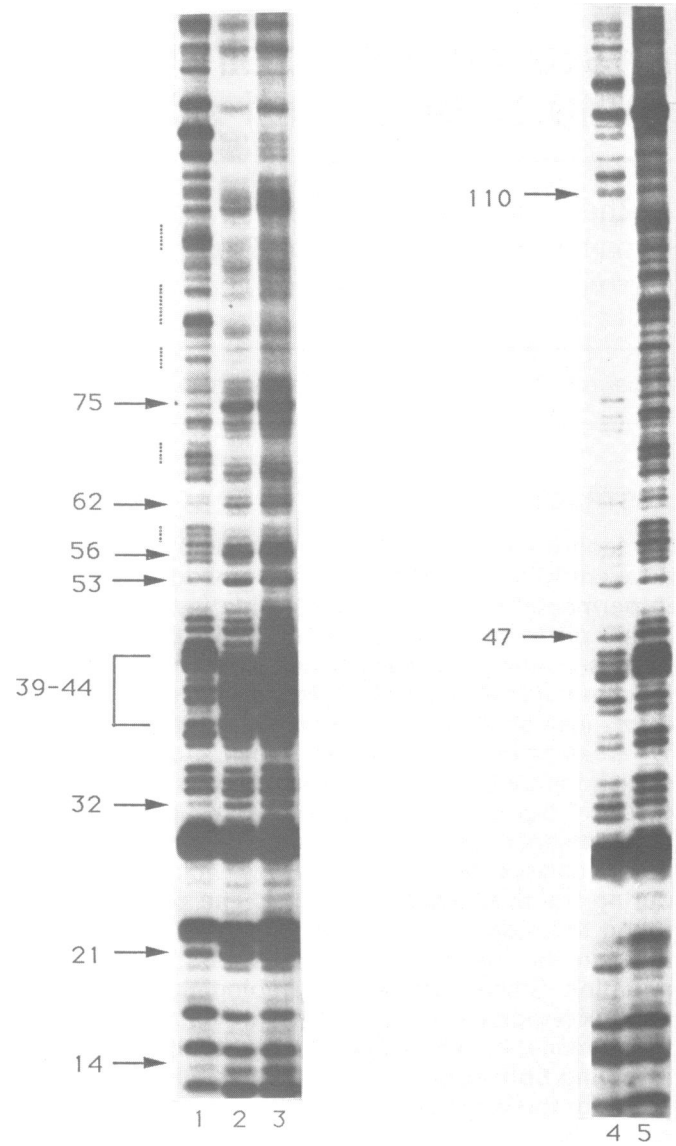

Figure 1. DNase I digestion pattern of the late mRNA template of the GC-box and AT-rich region at the late times of SV40 infection in permeabilized cells and nuclei. At 40 h post-infection, CV-1 cells were permeabilized and probed with approximately 0.1 mg/ml enzyme (lanes 2 and 3) and the naked DNA is digested by 10^{-5} mg/ml (lanes 1 and 5). The positions in lanes 2 and 3 that are hypersensitive to DNase I are labeled with arrows and a bracket; protected positions are marked by dashed lines. Lane 4 represents the DNase I digestion pattern of nuclei (for details see ref. 17) and the region between nt 47 and 110 is shown to be protected from DNase I digestion.

RESULTS

The method of probing SV40 nucleoprotein complexes involves detecting the sites of nuclease attack in the SV40 GC-box region in permeabilized infected cells. Lysolecithin is used to carry the nucleases deoxyribonuclease I (DNase I) and micrococcal nuclease (MNase) into CV-1 cells at 40 hours post-infection, which is well into the viral late phase. These enzymes attack the endogenous nucleoprotein complexes and introduce single strand breaks into the SV40 DNA. The viral DNA is then isolated and denatured, and the sites of nuclease attack in cells are determined by hybridization and extension *in vitro* of end-labelled primers flanking the region of interest (1). The permeabilized cell primer extension pattern is compared to that obtained by a similar analysis of naked DNA nicked *in vitro*. These patterns are compared for regions protected from nuclease attack, presumably due to bound proteins, and regions hypersensitive to nuclease attack, presumably due to factor-induced distortions in the DNA structure. Both of these features are displayed in the probing experiment shown in Figure 1.

Probing Indicates Higher Order Structures

Figure 1 compares the DNase I attack patterns under three conditions: on naked DNA *in vitro* (lanes 1 and 5), in permeabilized cells (lanes 2 and 3), and in isolated nuclei (lane 4). All three patterns result from digestion of the same DNA with the same enzyme, yet significant differences are apparent. In isolated nuclei (lane 4) the GC-box region from nt 47 to 110 is strongly protected from DNase I attack as evidenced by the lesser intensity of bands in that region compared to naked DNA samples (lane 5). This is essentially a repetition of a previous experiment that indicated factor binding to this region in isolated nuclei (17). Simple protection of this sort is typical of patterns seen using isolated GC-box binding proteins.

However, when DNase I is used to probe SV40 DNA in permeabilized cells (lanes 2 and 3) the pattern is much more complex, including positions that are protected (shown by dashed lines) as well as those that are hyperreactive to attack (shown by arrows and a bracket). Several protected bands in the GC-box region are marked with dashed lines adjacent to the *in vitro* digestion pattern displayed in lane 1. The bands protected beyond the GC-box region (upper part of lanes 1 and 2) are within the known binding sites for the enhancer factor AP-1; they will not be considered further since they are at the limit of reliable detections using this primer. Within the GC-box region a series of strong hyperreactive bands, shown by arrows and brackets, punctuate the protection pattern. Their appearance is the major difference from the continuous protection observed when nuclei are probed.

Previous studies have used lysolecithin to preserve nucleic acid synthesis that is usually lost upon preparation of nuclei (20,21). The procedure used here is designed according to previous analogous studies of SV40 infected CV-1 cells in which lysolecithin was used to preserve SV40 transcription initiation and SV40 DNA replication (19−21). Thus, we assume that this pattern of hyperreactive sites in permeabilized cells reflects a physiological structure that is disturbed when nuclei are prepared by the more drastic NP-40 lysis.

The strongest of these DNase I hypersites is centered near nt 42 (compare lanes 1 and 2), which is just at the early side of GC-box 1. A lighter exposure shows that several individual nucleotides in this region are hypersensitive to attack (not shown but listed in figure 6 below). Continuing towards the replication origin, other DNase hypersites appear at positions nt 32, nts 20/21, and nts 12/14. Within the GC-box region other sites appear at nts 53/56, nt 62 and nt 75. Note that these sites appear at approximately 10 base pair intervals (12/14, 21, 32, 42, 53/56, 62, 75). Probing beyond the borders of this region shows that the apparent periodicity does not extend beyond nt 1 on the early side or beyond the GC-boxes on the late side (not shown). Periodic DNase I hypersites are usually an indicator of nucleosomes and the results could indicate, for example, that a nucleosome was removed from the GC-box region during NP-40 lysis. However, the region encompassed here is too small, by a factor of two, to form a full nucleosome (26). The region is also within the nucleosome-free region of SV40 (27,28). Therefore, the hypersites appear to reflect some other type of nucleoprotein structure (29−32).

To probe the structure of this region in permeabilized cells further, we used another nuclease with a different mode of DNA recognition and cleavage. We have recently developed the use of micrococcal nuclease as a probe of nucleoprotein complexes *in vitro* (32) and in permeabilized cells (1). This enzyme is smaller than DNase I and recognizes the DNA backbone prior to single-strand cleavage (33); DNase I recognizes the DNA minor groove prior to cleaving one of the nearby backbone phosphodiesters (33,34). Both enzymes, however, have the common property of hypersensitive cleavage when their recognition site becomes prominently exposed as a consequence of protein-induced wrapping, looping, or bending of DNA.

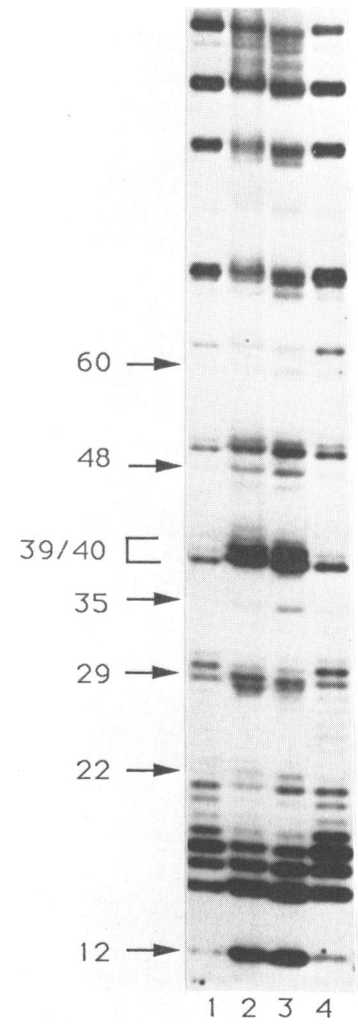

Figure 2. MNase digestion pattern of the GC-box and AT-rich region at the late times of SV40 infection in permeabilized cells. Infected cells were permeabilized and probed with approximately 250 units (lane 2) or 500 units (lane 3) of MNase and the naked DNA is digested by 0.01 units (lane 1) or 0.025 units (lane 4) of MNase in buffer C. The positions which are hypersensitive to MNase are labeled with arrows and brackets.

MNase was introduced into permeabilized cells in order to nick SV40 nucleoprotein complexes, and primer extension analysis of the nicked DNA *in vitro* revealed the attack pattern shown in Figure 2. This pattern resulted from use of the same primer, designed to read through the GC-box region, used in the DNase I probing displayed in Figure 1. The attack pattern from permeabilized cells (lanes 2 and 3) is quite similar to that obtained *in vitro* (lane 1) except that certain bands are hyperreactive to attack in cells.

The principal site of MNase hyperreactivity in permeabilized cells is coincident with the principal site of DNase I hyperreactivity in permeabilized cells, at nts 39/40 (compare lanes

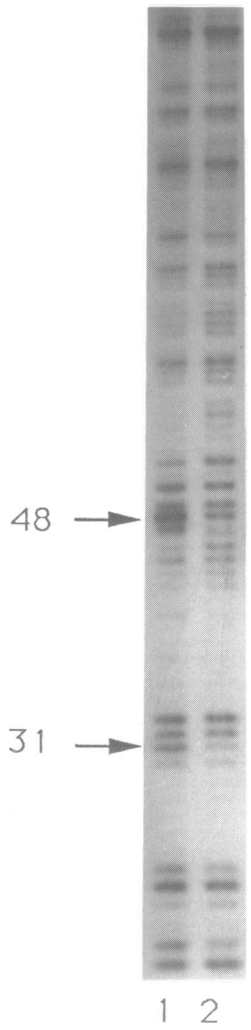

Figure 3. $KMnO_4$ modification pattern of the GC-box and AT-rich region. Lane 1, SV40 DNA in intact cells was modified with 10 mM $KMnO_4$. Lane 2, naked SV40 DNA was modified with 5 mM $KMnO_4$ *in vitro*.

2 and 3 with lane 1). Other hyperreactive sites flank the strongest site 9 base pairs into the GC-box region (nt 48) and 10 base pairs towards the early side (nt 29). Weaker hyperreactive sites flank these at nt 60, nt 22, and a strong site appears at nt 12. As was the case for the DNase I hypersites, most of the MNase hypersites appear at approximately 10 base pair intervals (nts 60, 48, 39, 29, 22, 12).

These nuclease probing results in permeabilized cells indicate the existence of a DNA structure in the region connecting the GC-boxes to the replication origin that is different from that occurring in naked DNA or isolated NP-40 nuclei. Periodicity of nuclease hypersensitive sites in nucleoprotein complexes is generally attributed to periodic exposure of potential cleavage sites on DNA as it assumes a curved path due to wrapping or looping (26,29–31). More extreme structural perturbations such as local DNA melting and very severe kinking can be detected by the reagent potassium permanganate ($KMnO_4$) (25,35–37). Strong hyperreactivity to this reagent indicates DNA melting, while weaker enhanced reactivity indicates local kinking or other structural perturbations. $KMnO_4$ may be applied directly to infected CV-1 cells and its attack pattern (on pyrimidines) may be determined by primer extension analysis (1,25,35,36). Figure 3 is a comparison of the $KMnO_4$ attack patterns on SV40 DNA in cells (lane 1) vs. on naked DNA *in vitro* (lane 2). The patterns are virtually identical except for positions of slightly enhanced reactivity *in vivo* at nts 31 and 48. These results confirm that the DNA structural modification is less drastic than DNA melting and suggest that it may involve occasional DNA kinks.

The Structure is Maintained by Elements on its Periphery

In some systems the DNA elements responsible for formation of unusual structures lie outside the perturbed DNA sequences themselves (29–31,36). As an initial test of this possibility we examined the properties of an SV40 deletion mutant (SVp7) that lacks 42 nucleotides between positions 32 and 73 (38). This mutant lacks the DNA sequences corresponding to the major hypersensitive site near nt 40 and removes several of the other periodic hypersites. The nucleotide sequences of SVp7 and wt between nts 32 and 42, where they are most different, are as follows:

wt - G T C A G C C A T G G
p7 - G G G G C G G G A T G

The 42 bp deletion corresponds to four helical turns of DNA (4 turns of 10.5 base pairs per turn) and thus preserves the phasing relationship between elements outside the region deleted. The virus is slightly impaired in function, giving two- or three-fold reduced yields (38). If the structure that is responsible for nuclease hypersensitivity is important and preserved in the virus, the periodic hypersensitivity itself should be preserved, despite the introduction of new DNA sequences at the sites of nuclease attack.

The DNase 1 digestion pattern of the mutant virus in situ is shown in figure 4, lanes 1 and 2. The result shows that this virus exhibits a non-uniform digestion pattern where regions of strong digestion alternate with regions of weak digestion (the strongly digested regions are bracketed to the left of the figure). This periodicity is not observed when naked mutant DNA is digested in vitro (lanes 3 and 4) and is thus a property of the cellular environment.

The result shows that the SVp7 mutant, which lacks nts 32 to 73, nevertheless displays an altered DNA structure somewhat similar to wild-type virus. Therefore, these nucleotides, which are within the region of altered structure in wild-type, are not essential for the formation of an in situ structure exhibiting periodic nuclease sensitivity. It should be noted, however, that although the sequences from nt 32 to 43, which include the major hypersites, are quite different in the mutant, beyond nt 43 the mutant and wt sequences are strongly similar due to the substitution of GC-boxes 5 and 6 for wild-type boxes 1 and 2. The extent of hypersensitivity of SVp7 is somewhat less than wild-type. Since SVp7 replicates less efficiently than wild-type, the lessened hypersensitivity could be due to a lower proportion of DNA in replication complexes. Alternatively, the changed DNA sequence could be intrinsically less sensitive to nuclease attack.

The nucleotide sequences to the early side of the region deleted in SVp7 are essential as they are responsible for SV40 T-antigen-dependent DNA replication. The region of altered structure detected in these experiments connects the essential T-antigen binding sites with the accessory GC-box and the distal enhancer control elements. Thus, it seemed possible that the altered structure would require T-antigen to form. We explored this possibility by use of the mutant SV40 virus tsA58. This virus has a temperature-sensitive T-antigen and cannot replicate at the

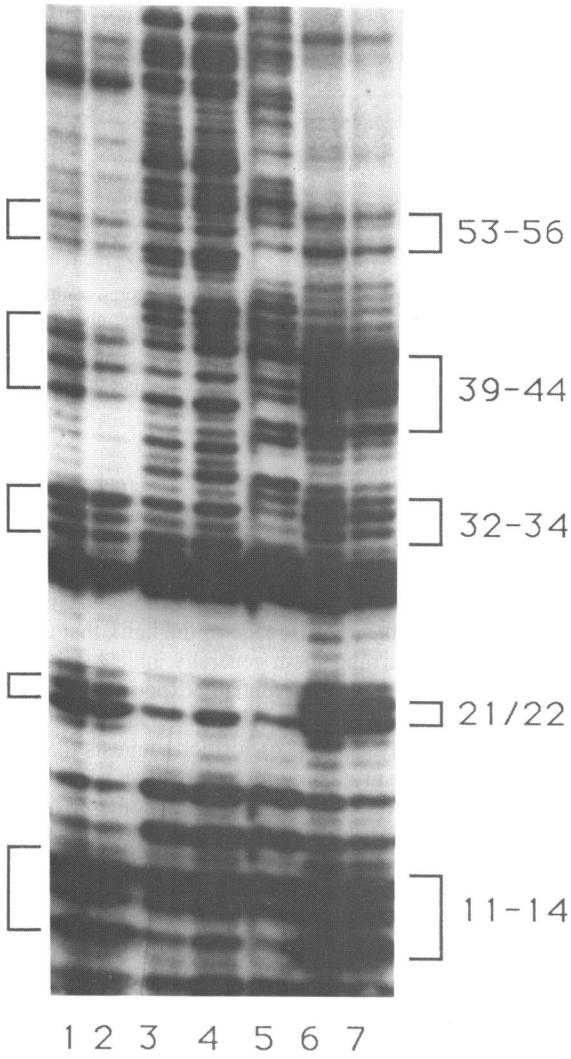

Figure 4. DNase I footprints on the late mRNA template strand of SVp7 mutant in the GC-box and AT-rich region in permeabilized cells. SVp7 DNA (lanes 3 and 4) or wt SV40 DNA (lane 5) is digested *in vitro* with approximately 10^{-5} mg/ml DNase I; SVp7 DNA (lanes 1 and 2) or wt SV40 DNA (lanes 6 and 7) in permeabilized cells is digested with approximately 0.1 mg/ml DNase I. The DNase I hypersensitive positions in wt SV40 and the corresponding positions in SVp7 mutant are shown by brackets.

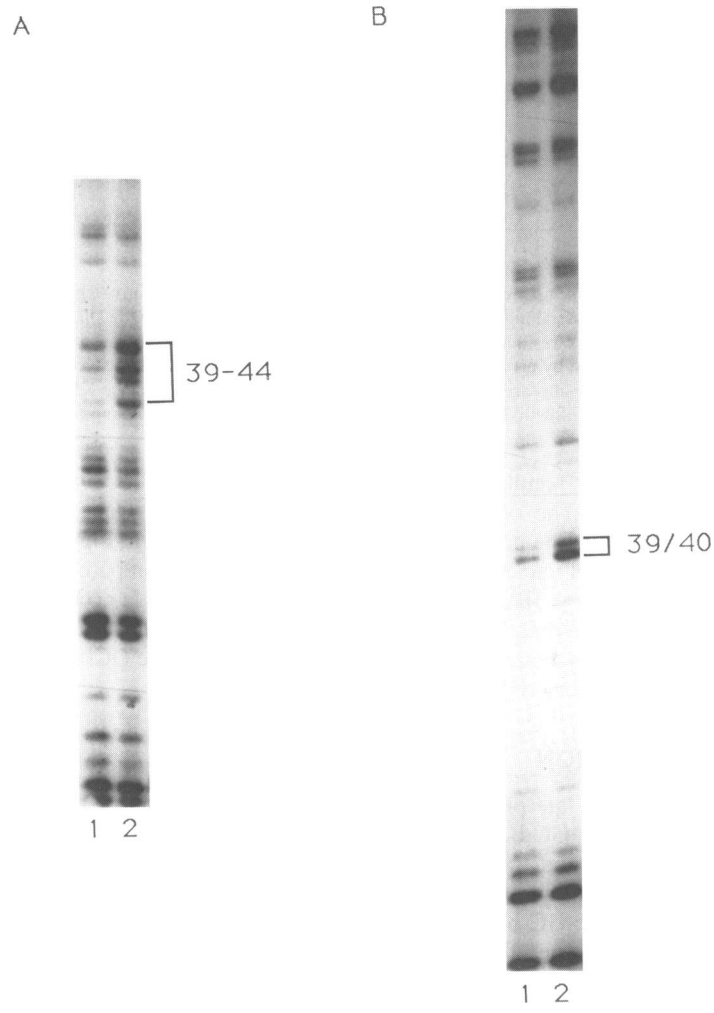

Figure 5. Comparison of the footprint of the T-antigen active complex and that of the T-antigen inactive complex. CV-1 cells were infected with tsA58 mutant and maintained at 32.5°C for 68 h, then the footprint of T-antigen active complexes was obtained by permeabilizing and probing the cells at 32.5°C, whereas that of T-antigen inactive complexes was obtained by subsequently incubating the 68 h post-infected cells at 41°C for another 5 h, followed by permeabilization and enzyme probing. (A) DNase I footprints of active (lane 2) and inactive T-antigen complexes (lane 1). Permeabilized cells were treated with 0.1 mg/ml DNase I. (B) MNase footprints of active (lane 2) and inactive T-antigen complexes (lane 1) produced by the use of primer 5230. Permeabilized cells were treated with 500 units of MNase.

non-permissive temperature (39). At elevated temperatures T-antigen fails to oligomerize and has reduced affinity for its SV40 DNA binding sites *in vitro* (40,41). The experiment is to grow the virus at the permissive temperature (32.5°C), allowing the structure to form, and then raise the temperature to 41°C to inactivate T-antigen, and probe whether the altered DNA structure, outside the T-antigen sites at ori, is maintained.

There are several technical complications that combine to reduce the resolution of the probing of tsA58 viruses. The virus grows quite slowly at the low permissive temperature and even with longer infection times less DNA is produced. Although the DNA sequence of the region probed is identical to wild-type SV40, the sequences near the primer hybridization site are somewhat different, which interferes with the analysis. The patterns obtained when tsA58 virus is probed with nucleases are shown in Figure 5.

Lanes 1 and 2 of Figure 5A compare the DNase I digestion patterns in cells containing inactive and active SV40 T-antigen, respectively. The samples probed in lane 1 differed only in that the infected cells were shifted to the non-permissive temperature for 5 hours prior to probing. The permeabilization and DNase I digestion was done by the usual treatment for 1−2 minutes at 37°C. Although the data are less extensive than those from wild-type virus, it is apparent that inactivating T-antigen leads to the disappearance of the major DNase I hypersensitive site near nt 40. That is, lane 1 and lane 2 are virtually identical except for the loss of intense bands near nt 40 in lane 1 which represents samples in which T-antigen was inactivated by culturing at the non-permissive temperature. This loss is not due to a loss of DNA binding since analogous experiments in nuclei (as in Fig. 1) show that the GC-boxes are still bound under these conditions (18). Neither is this loss due to the change in temperature itself since the hypersites remain in the wt SV40 pattern after a 5 hour shift to 41°C (not shown).

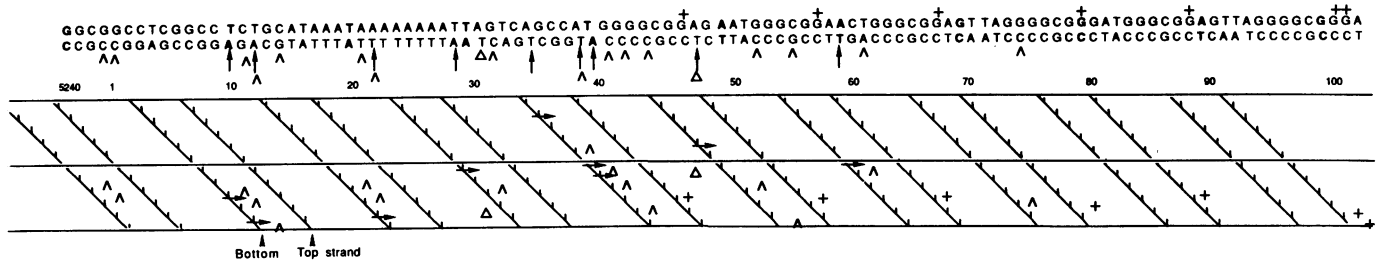

Figure 6. Helix map of DNase I, MNase and $KMn0_4$ hypersensitive sites. The DNA helix (10.5 base pairs per turn) is shown in planar representation such that the helix has cut along a single edge, unfolded and drawn flattened. Diagonal lines represent sugar-phosphate backbone, with tick marks being phosphate. DNase I hypersensitive residues are shown by carets in minor grooves because DNase I binds to the DNA minor grooves and then cleaves DNA. MNase hypersensitive sites are shown by arrows on the phosphate backbone because micrococcal nuclease binds to only one strand of DNA and then cleaves the phosphate bond. $KMn0_4$ hypersensitive sites are shown by triangles in the major grooves since $KMn0_4$ attacks pyrimidines at the 5,6 double bond in major grooves. Plus symbols represent sites of weak dimethyl sulfate hyperreactivity caused by SP-1 binding *in vitro* according to the data of Gidoni et al. (43).

A similar result is obtained when MNase is used as a probe (Fig. 5B). The only visible difference in samples from cells incubated at the non-permissive temperature (lane 1 in Fig. 5B) is the loss of nuclease hypersensitivity near nt 40 (compare with lane 2 in Fig. 5B). Based on the DNase I and MNase probing, we conclude that the full integrity of the nucleoprotein structure in the region that connects the replication origin to the GC-boxes and enhancers requires functional T-antigen.

DISCUSSION

During the late phase of the SV40 lytic cycle, DNA elements within the GC-box and enhancer elements influence SV40 replication and transcription initiation at remote sites (8–15). The roles of individual elements are quite complex since for example the GC-boxes normally influence DNA replication, but in their absence this function is taken over by the enhancers. Overall, the 400 base pair control region appears to act as a functional unit with critical elements at the periphery and redundant, accessory elements in between (7–15). The physical basis for these functional interactions involving several separated DNA elements is not known. Many proteins are likely to be involved in this regulation, but the only one known with certainty is the viral T-antigen which is directly required for DNA replication and also stimulates late mRNA synthesis both directly and indirectly (2–5).

One key result, shown in Figure 1, is that the GC-box region is strongly protected against nuclease digestion in isolated nuclei, but in permeabilized cells intermingled protection and hypersensitivity indicates that a more complex nucleoprotein structure exists. Because the permeabilization procedure does not involve cell lysis and is done directly on cultured cell monolayers, and because permeabilized cells but not nuclei preserve some ability to initiate SV40 nucleic acid synthesis (19–21), we assume that the permeabilized cell structure is the more physiologically relevant of the two. Apparently the lysis of cells and the subsequent isolation of nuclei disturbs the structure. Prior examples of structures involving such hyperreactive sites include nucleosomes and nucleoprotein complexes containing looped DNA (26,29–31).

A helix map analysis, shown in Figure 6, gives a clue concerning how this complex is held together. This map displays the positions of *in situ* attack along the full circumference of the DNA helix, by DNase I, MNase, and $KMn0_4$. Each hypersensitive site is represented by a symbol placed on the map according to how the reagent recognizes DNA; MNase (arrows) recognizes the backbone directly (33), DNase I (carets) recognizes the minor groove next to its cleavage site (33,34), and $KMn0_4$ (triangles) recognizes and cleaves pyrimidines through the major groove (35,37). Note that almost all the attack sites lie on the bottom half of the figure, indicating that the DNA is strongly exposed to attack on the specific face of the helix that the bottom half represents. This arrangement generally indicates that proteins are arrayed along one face, preferentially exposing the other DNA face to nuclease attack (29–32,34,42, see also below).

The helix map analysis (Fig. 6) further suggests that the GC-box binding factor is a protein with some DNA-binding properties in common with HeLa SP-1. This suggestion is based on an extension of the analysis of the data of Gidoni et al. (43) concerning SP-1 binding to the SV40 GC-boxes *in vitro*. SP-1 binds to one face of the GC-box region and further analysis of the array of dimethyl sulfate (weak) hypersites shows that they occur on the opposite helix face (see pluses in Fig. 6). In Figure 6, a line is drawn across the helix to separate the (upper) SP-1 bound face from the (lower) exposed face. Note that the face exposed when SP-1 binds *in vitro* is coincident with the exposed, hypersensitive face *in situ*. Thus, it seems likely that an SP-1-like factor is part of the protein complex occupying one face of the DNA. Another factor in the complex could be LOB (44), which binds *in vitro* to the AT-rich region between the SP-1 and the T-antigen sites and causes a DNA bend that is just to the Early side of the major nuclease hypersensitive site detected in these *in situ* probing studies.

Some of the elements that determine the nucleoprotein structure can be tentatively identified from these results. The identification is based on the effect of mutants on the strong, hypersensitive site near nt 40 that accompanies structure formation in permeabilized cells, but not in nuclei. T-antigen acting at the replication origin appears to be one important determinant, since when replication is inhibited by temperature inactivation of T-antigen in tsA58 virus, the major hypersensitive site (nts 38–42) in the connector region disappears. This hypersensitive site is not caused by T-antigen alone, since it is not induced by T-antigen *in vitro* and lies outside the main T-antigen DNA binding sites which are closer to the origin region (45). Nor is this site induced in reconstructed systems containing both T-antigen and bound SP-1 (46) or by LOB alone or by LOB and T-antigen (44). Obviously, factors remain to be identified. The DNA within the hypersensitive site itself does not appear to be a critical determinant since the hypersensitivity remains in the SV-P7 mutant which substitutes heterologous sequences at the site. Taken together, these data indicate that the determinants that cause the

major hypersensitive site are outside the site itself and involve multiple factors.

The major and minor nuclease-sensitive sites associated with this structure constitute a periodic array, which is an indicator of DNA wrapping or looping (26,29–31). Wrapping or looping causes the DNA to bend or kink as it assumes a sharply curved path; this in turn allows nucleases increased access to the DNA at the kink points on the outside face of the DNA (32–34). Such structures have been recently shown to be important in replication (47), transcription (30,32) and recombination (31,48,49) of E. Coli DNA. By analogy the most likely model for the structure of this 75 base pair region in permeabilized cells involves the DNA curving or wrapping around bound proteins, causing the outside face to become hyperreactive to attack. The exposed face may be severely kinked near nt 40, where the strongest DNA distortion occurs. The phased, higher order structure near the replication origin may even be more extensive than indicated here, as for example exists in prokaryotic replication origins (47), since mutants that do not preserve appropriate spacing between elements involve significant loss of function (6,22,50). In nuclei, the superstructure is disrupted causing the disappearance of the hyperreactive attack sites, while retaining DNA binding by some of the factors. This would also be expected to be true in isolated SV40 minichromosomes which are generally derived from nuclei or by other harsh lysis treatments (27,28).

The elements within this large nucleoprotein complex are multifunctional, influencing DNA replication as well as RNA transcription at several sites (10–15). In these experiments only 10% of the total intracellular DNA is nicked, corresponding principally to the nuclease sensitive minichromosomes typically associated with SV40 nucleic acid synthesis (see 17 for a discussion). Although the experiments presented in this paper provide a rationale for how remote SV40 sequences can interact, they cannot indicate which of the functions are affected by formation of the extensive nucleoprotein structure. Aphidicolin, if added early, prevents the assembly of this structure, but this does not indicate its function since the drug inhibits only enyzmatic synthesis of DNA (18). Similarly, studies with alpha amanitin (1) are uninformative since this drug acts at the elongation of already initiated RNA. Previously, we made the suggestion that the complex detected may be involved in repression of replication (18) but probing experiments alone cannot definitively test such suggestions. Ultimately, one needs to reconstruct the regulatory apparatus *in vitro*, and the *in situ* results described here should be a very valuable guide towards physiologically appropriate reconstruction.

ACKNOWLEDGEMENTS

This research was supported by a grant from the National Science Foundation (DMB85-12033).

REFERENCES

1. Zhang, L. and Gralla, J.D. (1989) Genes and Dev. **3**, 1814–1822.
2. Alwine, J.C., Reed, S.I., and Stark, G.R. (1977) J. Virol. **24**, 22–27.
3. Rio, D.C. and Tjian, R. (1983) Cell **32**, 1227–1240.
4. Tegtmeyer, P. (1972) J. Virol. **10**, 591–598.
5. Tjian, R. (1981) Cell **26**, 1–2.
6. Fromm, M. and Berg, P. (1982) J. Mol. Appl. Gen. **1**, 457–481.
7. Ayer, D.E. and Dynan, W.S. (1988) Mol. Cell. Biol. **8**, 2021–2033.
8. DePamphilis, M.L. (1988) Cell **52**, 635–638.
9. Hartzell, S.W., Byrne, B.J., and Subramanian, K.N. (1984) Proc. Natl. Acad. Sci. USA **81**, 23–27.
10. Barrera-Saldana, H., Takahashi, K., Vigneron, M., Wildeman, A., Davidson, I., and Chambon, P. (1985) EMBO J. **4**, 3839–3849.
11. Ernoult-Lange, M., Omilli, F., and May, E. (1987) Nucl. Acids Res. **15**, 8177–8193.
12. Hertz, G.Z. and Mertz, J.E. (1986) Mol. Cell. Biol. **6**, 3513–3522.
13. Hertz, G.Z. and Mertz, J.E. (1988) Virology **163**, 579–590.
14. Lee-Chen, G., and Woodworth-Gutai, M. (1986) Mol. Cell. Biol. **6**, 3086–3093.
15. Li, J.J., Peden, K.W.C., Dixon, R.A.F., and Kelley, T. (1986) Mol. Cell. Biol. **6**, 1117–1128.
16. Jones, N.C., Rigby, P.W.J., and Ziff, E.B. (1988) Genes and Dev. **2**, 267–281.
17. Buchanan, R.L. and Gralla, J.D. (1987) Mol. Cell. Biol. **7**, 1554–1558.
18. Buchanan, R.L. and Gralla, J.D. (1989) J.Vir. **64**, 347–353.
19. Contreras, R. and Fiers, W. (1981) Nucl. Acids Res. **9**, 215–236.
20. Miller, M.R., Castellot, J.J., Jr., and Pardee, A.B. (1978) Biochemistry **17**, 1073–1080.
21. Sarkar, N., List, J.F. and Banfalvi, G. (1987) Eur. J. Biochem. **168**, 263–268.
22. Innis, J.W. and Scott, W.A. (1983) Mol. Cell. Biol. **3**, 2203–2210.
23. Hirt, B. (1967) J. Mol. Biol. **26**, 365–369.
24. Gralla, J.D. (1985) Proc. Natl. Acad. Sci. USA **82**, 3078–3081.
25. Sasse-Dwight, S. and Gralla, J.D. (1989) J. Biol. Chem. **264**, 8074–8081.
26. Drew, H.R. and Travers, A.A. (1985) J. Mol. Biol. **186**, 773–790.
27. De Bernadin, W., Koller, T., and Sogo, J.M. (1986) J. Mol. Biol. **191**, 469–482.
28. Griffith, J.D. (1975) Science **187**, 1202–1203.
29. Hochschild, A. and Ptashne, M. (1986) Cell **44**, 681–687.
30. Raibaud, O., Vidal-Ingigliardi, D., and Richet, E. (1989) J. Mol. Biol. **205**, 471–485.
31. Salvo, J.J. and Grindley, N.D. (1988) EMBO J. **7**, 3609–3616.
32. Zhang, L. and Gralla, J.D. (1989) Nucl. Acids Res. **17**, 5017–5028.
33. Drew, H.R. (1984) J. Mol. Biol. **176**, 535–557.
34. Suck, D., Lahm, A., and Oetner, C. (1988) Nature **332**, 464–468.
35. Borowiec, J.A., and Hurwitz, J. (1988) EMBO J. **7**, 3149–3158.
36. Borowiec, J.A., Zhang, L., Sasse-Dwight, S., and Gralla, J.D. (1987) J. Mol. Biol. **196**, 101–111.
37. Hayatsu, H. and Ukita, T. (1967) Biochem. Biophys. Res. Commun. **29**, 556–561.
38. Buchanan, R.L. and Gralla, J.D. (1989) Biochemistry, in press.
39. Khoury, G. and May, E. (1977) J. Virol. **23**, 167–176.
40. Fanning, E., Bowak, B., and Burger, C. (1981) J. Virol. **37**, 92–102.
41. Wilson, V.G., Tevethia, M.J., Lewton, B.A., and Tegtmeyer, P. (1982) J. Virol. **44**, 458–466.
42. Borowiec, J.A. and Gralla, J.D. (1986) Biochemistry **25**, 5051–5057.
43. Gidoni, D., Dynan, W.S., and Tjian, R. (1984) Nature **312**, 409–413.
44. Baur, C.P. and Knippers, R. (1988) J. Mol. Biol. **203**, 1009–1019.
45. Borowiec, J.A. and Hurwitz, J. (1988) Proc. Natl. Acad. Sci. USA **85**, 64–68.
46. Mitchell, P.J., Wang, C., and Tjian, R. (1987) Cell **50**, 847–861.
47. Bramhill, D. and Kornberg, A. (1988) Cell **52**, 743–755.
48. Goodman, S.D. and Nash, H.A. (1989) Nature **341**, 251–254.
49. Snyder, U.K., Thompson, J.F. and Landy, A. (1989) Nature **341**, 254–257.
50. Brady, J., Loeken, M.R., and Khoury, G. (1985) Proc. Natl. Acad. Sci. USA **82**, 7299–7303.